Review of the Electronic Structure of Molecular Oxygen

J. S. Morrill[1], M. L. Ginter[2], B. R. Lewis[3] and S. T. Gibson[3]
[1]E. O. Hulburt Center for Space Research, Naval Research Laboratory, Washington DC 20375-5352
[2]IPST, University Of Maryland, College Park, MD 20742,
[3]The Australian National University, Canberra, ACT 0200, Australia

1 Introduction

The spectra and electronic structures of molecular oxygen play dominant roles in both the absorption of solar radiation and the emission spectra observed in the airglow and aurora. The last comprehensive review for O_2 was by Krupenie [1972]. Subsequently, there have been numerous treatments of many facets of the ground and lower excited electronic states up to and including the $B\,^3\Sigma_u^-$ state, the upper state of the Schumann-Runge system. While a summary of this information is presented, emphasis here is on the state of knowledge of the complex electronic structures which arise from the interaction between the Rydberg-Rydberg and Rydberg-valence states of both *u* and *g* symmetries in the region above the $B\,^3\Sigma_u^-$ state. These data are part of a comprehensive review of the electronic structure and spectra of O_2 which is currently nearing competition [Morrill et al., 1998].

2 Molecular Orbital Configurations

Selected configurations and associated electronic states are shown below.

O_2 Valence States

- Ground state configuration - Electronic States
  $(1\sigma_g)^2\,(1\sigma_u)^2\,(2\sigma_g)^2\,(2\sigma_u)^2\,(3\sigma_g)^2\,(1\pi_u)^4\,(1\pi_g)^2$ - $X^3\Sigma_g^-$, $a^1\Delta_g$ and $b^1\Sigma_g^+$.

- Excited state configurations - Electronic States
  $(1\sigma_g)^2\,(1\sigma_u)^2\,(2\sigma_g)^2\,(2\sigma_u)^2\,(3\sigma_g)^2\,(1\pi_u)^3\,(1\pi_g)^3$ - $B^3\Sigma_u^-$ ($^1\Sigma_u^\pm$, $^3\Sigma_u^+$, $^1\Delta_u$, and $^3\Delta_u$)

O_2 Rydberg states

- O_2^+ ion ground state configuration - Electronic State
  $(1\sigma_g)^2\,(1\sigma_u)^2\,(2\sigma_g)^2\,(2\sigma_u)^2\,(3\sigma_g)^2\,(1\pi_u)^4\,(1\pi_g)^1$ - $X\,^2\Pi_g$

- O_2 Rydberg states built on ion core, nl-complexes: $[X\,^2\Pi_g]nl\lambda_s$

Typical Rydberg states resulting from the addition of various $nl\lambda_s$ orbitals to the ground state of O_2^+ are shown in table 1.

Table 1. Electronic states associated with $[X^2\Pi_g]$ $ns\sigma_g$, $np\sigma_u$, and $nd\lambda_g$ Rydberg configurations[1].

Rydberg orbital	Configuration Type	Possible States
$ns\sigma_g$	$\pi_g\ \sigma_g$	$^{1,3}\Pi_g$
$np\sigma_u$	$\pi_g\ \sigma_u$	$^{1,3}\Pi_u$
$np\pi_u$	$\pi_g\ \pi_u$	$^{1,3}\Sigma_u^{\pm}$, $^{1,3}\Delta_u$
$nd\sigma_g$	$\pi_g\ \sigma_g$	$^{1,3}\Pi_g$
$nd\pi_g$	$\pi_g\ \pi_g$	$^{1,3}\Sigma_g^{\pm}$, $^{1,3}\Delta_g$
$nd\delta_g$	$\pi_g\ \delta_g$	$^{1,3}\Pi_g$, $^{1,3}\Phi_g$

[1] $[X^2\Pi_g]$ represents the ground state of O_2^+ which has a single π_g orbital outside closed subshells.

Work by Lewis et al. [1995] and England et al. [1995, 1996 a, b] has examined the details of many of the O_2 Rydberg states of *u*-symmetry, including the $np\sigma_u$ $^3\Pi_u$ Rydberg states with n=3-7 (e.g. $F\,^3\Pi_u$ and $F'^3\Pi_u$.) and $np\pi_u$ $^3\Sigma_u^-$ Rydberg states for n=3-5. These Rydberg states couple with the $^3\Pi_u$ and $^3\Sigma_u^-$ valence states to give rise to the complex adiabatic potential-energy curves. The analysis of such interactions has employed a coupled Schrodinger Equation (CSE) model which empirically models the off-diagonal elements of the Hamiltonian

$$\begin{bmatrix} H_{11} & H_{12} \\ H_{21} & H_{22} \end{bmatrix} \begin{bmatrix} X_1^N \\ X_2^N \end{bmatrix} = E \begin{bmatrix} X_1^N \\ X_2^N \end{bmatrix},$$

which leads to coupled equations

$$(H_{11} - E)X_1^N = -H_{12}\, X_2^N$$
$$(H_{22} - E)X_2^N = -H_{21}\, X_1^N$$

which are solved numerically.

Currently we are examining the Rydberg states of *g*-symmetry. Diabatic potential energy curves for some experimentally observed gerade Rydberg states and selected overlapping valence states shown in figure 2 and provide a example of our results. The Rydberg-valence interactions between the states in figure 2 produce anomalous energy level patterns and spectra. Preliminary analysis [Morrill et al., 1997] of the $d^1\Pi_g$, $2^1\Pi_g$, $1^1\Pi_g$ interaction using a CSE model leads to the rotational term diagram in figure 3. Use of these term energies (based on the v=0 of the $X\,^3\Sigma_g^-$) and the intensity relations in Bray and Hochstrasser [1976], produces a synthetic spectrum of the $d\,^1\Pi_g$ - $a\,^1\Delta_g$ (2,0) band which fits closely the experimental observations (see for example figures 4 and 5). Although the intensities of several features in figure 4 require further refinements the energies and major spectral features are well reproduced. At the present time, many other anomalies involving the $d\,^1\Pi_g$ and $C\,^3\Pi_g$ states, as well as higher energy *g*-Rydberg states, have been explained using similar procedures.

References

[1] Bray, R. G., and R. M. Hochstrasser, *Molec. Phys.*, **31**, 1199 (1976)
[2] England, J. P., B. R. Lewis, and S. T. Gibson, *J Chem Phys*, **103**, 1727 (1995)
[3] England, J. P., B. R. Lewis, S. T. Gibson, and M. L. Ginter, *J Chem Phys*, **104**, 2765 (1996a)
[4] England, J. P., B. R. Lewis, and M. L. Ginter, *J Chem Phys*, **105**, 1754 (1996b)
[5] Johnson, R. D., G. R. Long, and J. W. Hudgens, *J Chem Phys*, **87,** 1977 (1988)
[6] Krupenie, P. H. , *J. Phys. Chem. Ref. Dat*., **1**, 423 (1972)
[7] Lewis, B. R., S. S. Banerjee, and S. T. Gibson, *J Chem Phys*, **102**, 6631 (1995)
[8] Lewis, B. R., S. S. Banerjee, and S. T. Gibson, *J Chem Phys*, **102**, 6631 (1995)
[9] Morrill J. S., M. L. Ginter, B. R. Lewis, and S. T. Gibson, to be submitted to *J. Phys. Chem. Ref. Dat*. (1998)
[10] Morrill J. S., M. L. Ginter, B. R. Lewis, and S. T. Gibson, submitted to *J Chem Phys*. (1997)
[11] Partridge, H., C. W. Bauschlicher, S. R. Langhoff, and P. R. Taylor, *J Chem Phys*, **95**, 8292 (1991)
[12] Saxon, R. P., and B. Liu, *J Chem Phys*, **67**, 5432 (1977)

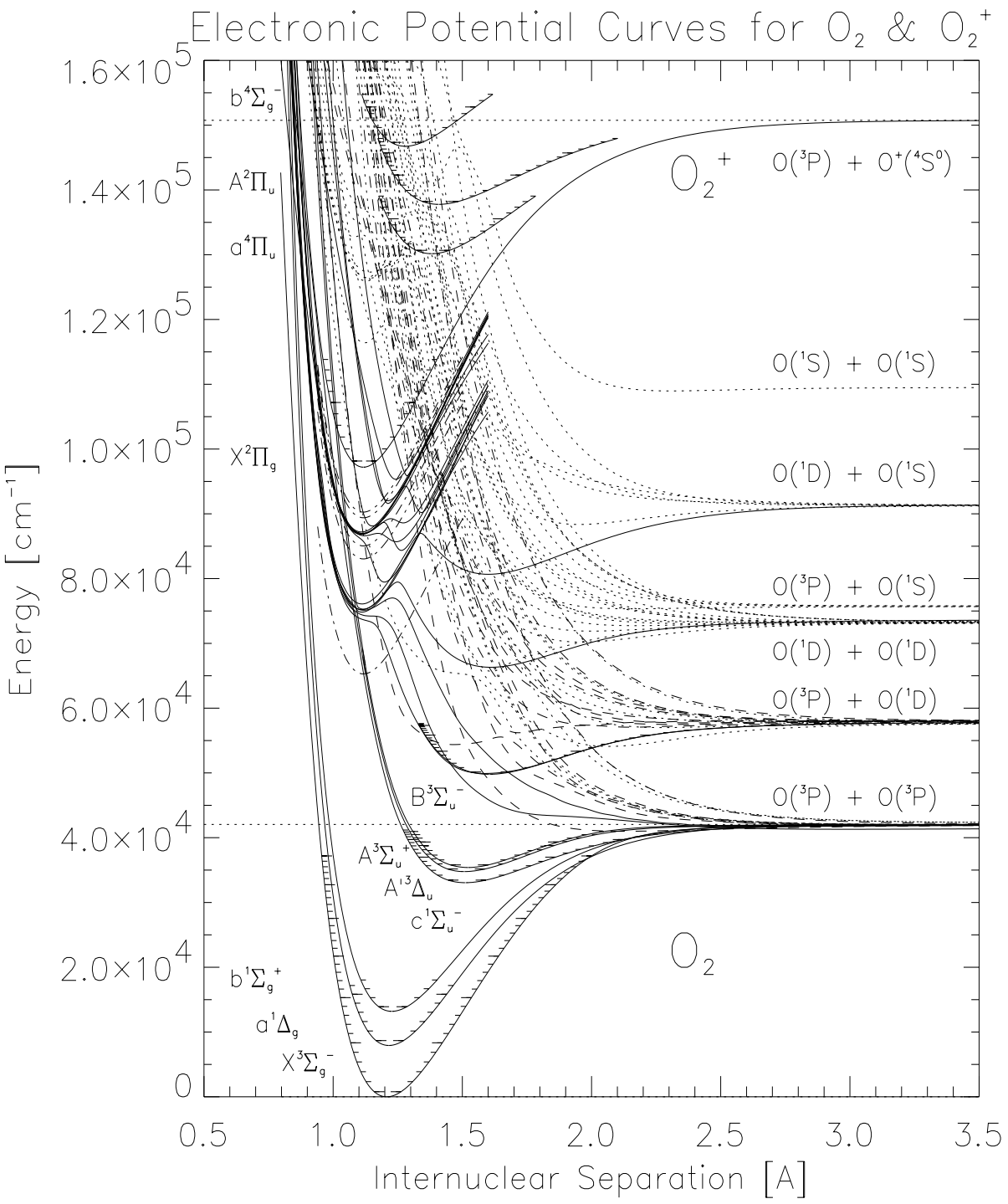

Figure 1 displays a complete collection of the lower lying valence electronic states of O_2 and a number of the adiabatic potential energy curves which result from Rydberg-valence interactions. The states with the vibrational levels indicated by tick marks were calculated by the RKR method. The dotted curves are the theoretical potentials generated by Saxon & Liu [1977] and the dashed curves are from Partridge et al. [1991] or Partridge [Private Comm.]. The dot-dash curves are diabatic representations of the $nl\lambda_g$ Rydberg states with $n \geq 5$.

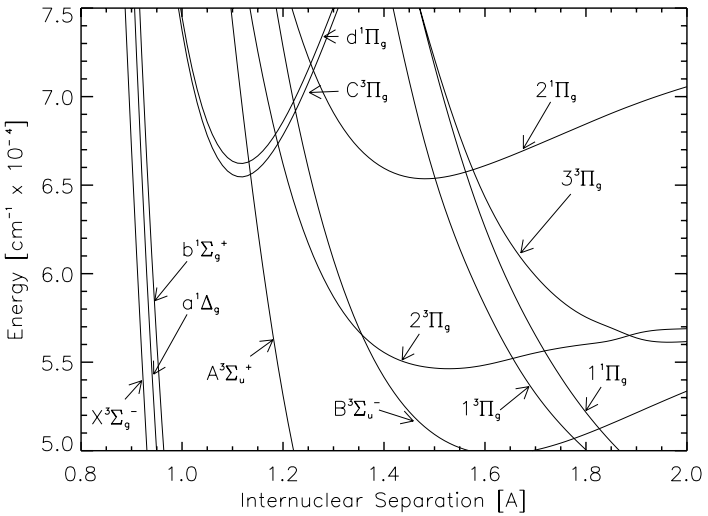

Figure 2: Diabatic 3sσ_g *d* $^1\Pi_g$ and *C* $^3\Pi_g$ Rydberg states and nearby valence states.

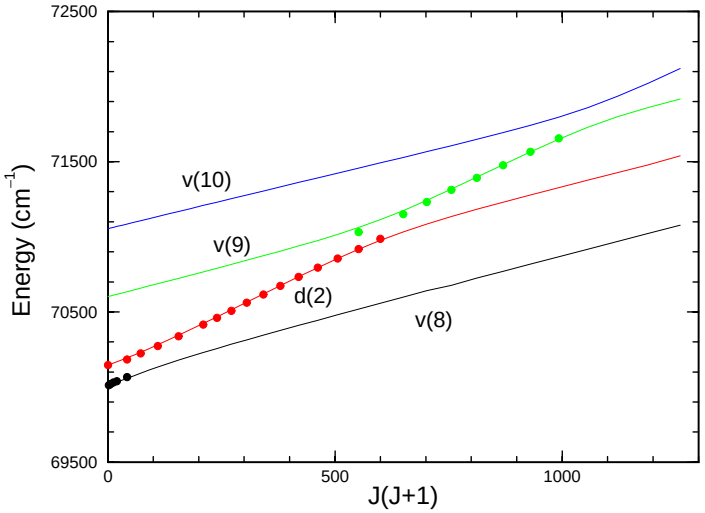

Figure 3: Rotational term values for the interacting $d^1\Pi_g$ and $2^1\Pi_g$ states with vibrational numbering in '( )'.

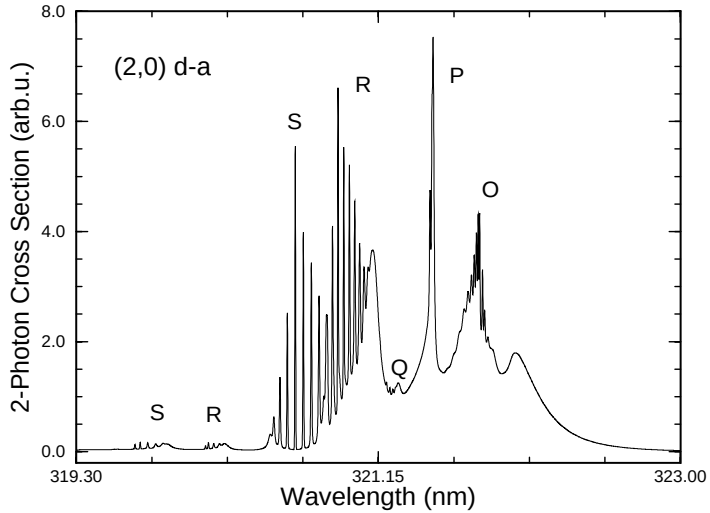

Figure 4: Synthetic $d^1\Pi_g$ - $a^1\Delta_g$ (2,0) band showing the effects of the perturbations indicated in figure 3.

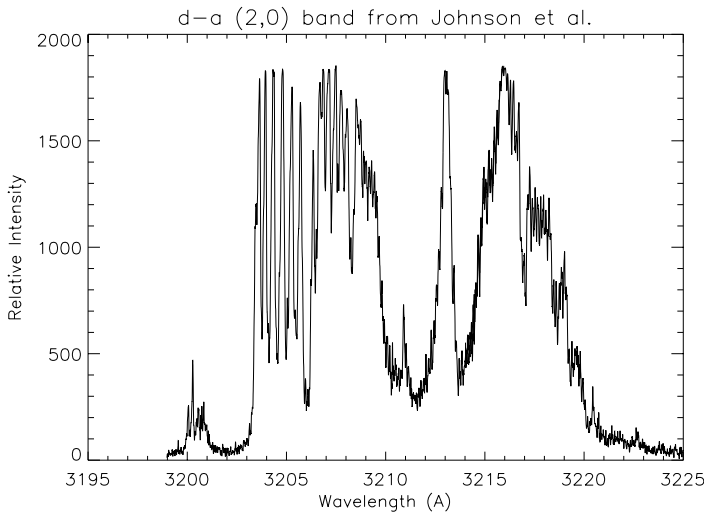

Figure 5: Observed 2+1 REMPI spectrum of the $d^1\Pi_g$ - $a^1\Delta_g$ (2,0) band measured by Johnson et al. [1988].